23rd ABCM International Congress of Mechanical Engineering
December 6-11, 2015, Rio de Janeiro, RJ, Brazil

NORMAL BOUNDARY INTERSECTIONAND ROBUST OPTIMIZATION APPLIED TO F_Z MACHINING FORCE COMPONENT IN HELICAL MILLING PROCESS

Aline Cunha Alvim
Robson Bruno Dutra Pereira
Universidade Federal de São João del-Rei. Campus Santo Antônio - Praça Frei Orlando, 170, Centro,São João del-Rei, MG. 36.307-352.
ca.aline@yahoo.com.br; robsondutra@ufsj.edu.br

João Roberto Ferreira
Anderson Paulo de Paiva
Universidade Federal de Itajubá, Instituto de Engenharia de Produção e Gestão, Avenida BPS, 1303, Itajubá, MG. 37500-903.
jorofe@unifei.edu.br; andersonppaiva@unifei.edu.br

Frederico Ozanan Neves
Universidade Federal de São João del-Rei. Campus Santo Antônio - Praça Frei Orlando, 170, Centro, São João del-Rei, MG. 36.307-352.
fred@ufsj.edu.br

Abstract.*The present study aimed to analyze the modeling and optimization of F_z machining force component obtained by helical milling process on a Al7075. It was used a central composite design, considering process and noise parameters in order to enable the robust parameter problem and model the mean and the variance functions of the F_z response. The normal boundary intersection and the mean square error approach were used to obtain a set of satisfactory Pareto solutions for both mean and variance functions of F_z. The noise variable considered was the tool length, once the geometry of the part requires a specific value of tool length while machining cavities. By these means, the tool length cannot be considered a process variable, because it does not depend on the choice of the experimenter. Through the suggested methodology, the F_z machining force component has been optimized, contributing mostly, in percentage terms, to the machining force, making robust the noise variation.*

Keywords:*helical milling, machining force component F_z, robust parameter design, dual response surface, normal boundary intersection approach.*

1. INTRODUCTION

Drilling is one of the most important metal cutting operations and often carried out as one of the last steps in the manufacturing production of a part, when already added considerable economic value to the product. Thus, reliability and robustness are indispensable to secure the considerable value already provided (Tonshoff*et al.*,1994). Although much used in the hole-making process, drilling has some disadvantages such as inefficiency on chips evacuation and effective heat dissipation in holes. Frictions between tool, chip and part is likely to negatively influence on the dimension accuracy and surface finish of the machined hole, which can lead on tool failure (Iyer*et al.,* 2007; Tonshoff*et al.*, 1994).

An alternative for drilling is Helical Milling. Helical Milling confers greater machining accuracy and surface finish. This method has some advantages as low burr formation, low cutting forces and good chip transportation(QIN et al., 2012).Helical Milling is a process which tool executes a helical path and a rotational movement around its own axis. The helical path has the advantage to reduce cutting efforts on axial direction, in addition to obtain holes with different diameters without changing the tool (Denkena *et al.*, 2008).

Helical milling first appeared in hole-making for aeronautical materials and is widely used in manufacturing industry nowadays(Li and Liu, 2013).Sasahara*et al.* (2008)used the aluminum alloy A5052 in order to verify the helical milling hole-making process with MQL. Bhattacharyya *et al.*(2010) and Li and Liu (2013)tested analytic models aimed to borehole machining on helical milling of aluminum alloy 6061-T6 and 7076-T6, respectively. Yicai*et al.* (2011) studied the big pitch influence on cutting force and bore quality on a helical milling hole-making of aerospace aluminum alloy 6061.

The aim of the present study was to analyze the modeling and optimization of F_z cutting force componentobtained by helical milling process on Al alloy 7075. It was used a central composite design, considering process and noise parameters to enable the robust parameter design, modeling mean and variance functions of the response. The normal boundary intersection and mean square error approach was used to obtain a set of Pareto optimal solution for mean and variance of F_z. The noise variable considered was the tool length, once the geometry of the part requires a specific value of tool length while machining cavities. By these means, the tool length cannot be considered a process variable, because it does not depend on the choice of the experimenter.

The $F_z$was chosenas outcome because it is the most challenging machining force component, especially in drilling process, and needs to be minimized, guaranteeing tool integrity and good results in terms of dimensional, geometrical and microgeometrical quality of the hole. Other variables are actually in study and the results will be published in future works. It is important to emphasize that the F_z do not correspond to the thrust force F_f as in drilling process, once in helical milling process the feed is not on axis direction, but has a helical trajectory. The levels of F_x and F_y machining forces components are lagged between themselves and lower than F_z. They can be quantitatively availed as Eq. (1), and will be treated in a future work in a multivariate analysis.

$$F_{xy} = \sqrt{F_x^2 + F_y^2} \tag{1}$$

1.1 Helical millingkinematics

While on drilling process the bore diameter is defined by the drill diameter, in helical milling the bore diameter comes from the combination of the tool diameter and the diameter of the helical path (Denkena*et al.*, 2008).According to Yicai *et al.* (2011), in the hole milling the tool executes three movements simultaneously. Rotation around its own axis, feed along axis direction, and revolution around hole axis.

Speeds related to the process are cutting speed (v_c), in m/min, which is associated to tool diameter and tool rotation around its own axis; and feed speed (v_f), in mm/min, which is associated to speed on the tool center point, i. e., the speed which the tool covers the helical path. Helical feed speed (v_f) can be decomposed into axial feed speed (v_{fha}) and tangential feed speed (v_{fht}), according to Eq. (2). Hole and helix diameter are also important to v_{fht}calculation, according to Eq. (3), (4) and (5). Figure 1 illustrate above-mentioned parameters.

$$v_f = \sqrt{{v_{fha}}^2 + {v_{fht}}^2} \tag{2}$$

$$v_{fha} = f_{za} \cdot z \cdot n \tag{3}$$

$$v_{ft} = f_{zt} \cdot z \cdot n \tag{4}$$

$$v_{fht} = v_{ft} \frac{D_h}{D_B} \tag{5}$$

On Eq. (3), (4) and (5), v_{ft} is the tangential feed speed (mm/min);f_{za} is the axial feed per tooth (mm/revolution);f_{zt} is the tangential feed per tooth (mm/revolution);z is the number of teeth;n is the revolution per minute (RPM);D_h is the helix diameter (mm);and D_B is thebore diameter (mm). The cutting depth (a_p) can be defined by Eq. (6), considering helix angle (α) defined by Eq.(7).

$$a_p = \tan(\alpha) \cdot \pi \cdot D_h \tag{6}$$

$$\alpha = \arctan\left(\frac{v_{fha}}{v_{fht}}\right) \tag{7}$$

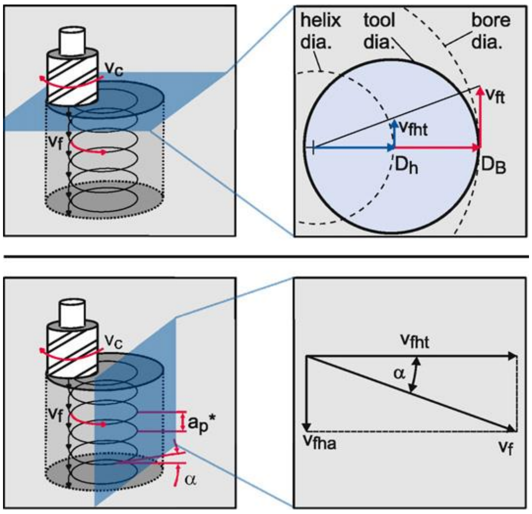

Figure 1. Cutting parameters(Denkena*et al.*, 2008)

2. ROBUST PARAMETER DESIGN WITH COMBINED ARRAY DESIGN

Robust Parameter Design – RPD, is a set of techniques determining the optimal levels of control factors that decrease the sensitivity of the process to noise factors variation, thus increasing the robustness of the process(Ardakani and Noorossana, 2008). This study used the Design of Experiments – DOE methodology. According to Myers and Montgomery (1995), the DOE methodology is a statistical approach that focuses on the design of experiments for generation of data suitable for an effective statistical analysis.According to the authors, the interactions between control and noise factors are crucial on Robust Problem Design – RPD. Therefore, it is logical the need of a model for the response that includes both control and noise factors and their interactions. The design containing both control and noise factors is known as Combined Array Design.

The general problem RPD-RSM consists on the schedule of an experimental design that considers noise factors as control factors and removes the axial points related to noise factors out of the design. Thus, by means of Ordinary Least Squares - OLS or Weighted Least Squares – WLS a polynomial surface $y(x,z)$can be obtained and then, the mean and the variance surface for this response, considering the interactions between control and noise factors (Ardakani and Noorossana, 2008; De Paiva *et al.*, 2014). These surfaces are called Dual Response Surface – DRS and they are a class of RSM problems(De Paiva*et al.*, 2014). Equations (8), (9) and (10)illustrate the model of response, the mean model for response and the variance model for response, respectively. Where k and r are the number of control and noise factors, respectively; the parametersβ and $\gamma$are called regression coefficients for control and noise factors, respectively; x represents the control factors and z the noise factor; and ε the sum of the squares of the errors.

$$y(x,z) = \beta_0 + \sum_{j=1}^{k} \beta_j x_j + \sum_{i} \sum_{<j} \beta_{ij} x_i x_j + \sum_{j=1}^{k} \beta_{jj} x_j^2 + \sum_{i=1}^{r} \gamma_i z_i + \sum_{i=1}^{k} \sum_{j=1}^{r} \delta_{ij} x_i z_j + \varepsilon \tag{8}$$

$$E_z[y(x,z)] = \beta_0 + \sum_{j=1}^{k} \beta_j x_j + \sum_{i} \sum_{<j} \beta_{ij} x_i x_j + \sum_{j=1}^{k} \beta_{jj} x_j^2 \tag{9}$$

$$V_Z[y(x,z)] = \sum_{i=1}^{r} \left[\frac{\partial y(x,z)}{\partial z_i} \right]^2 \sigma_{z_i}^2 + \sigma^2 \tag{10}$$

3. NON-LINEAR OPTIMIZATION

The functions explained on the Eq. (9) and (10) may be optimized simultaneously considering different methods. The non-linear optimization was applied to RSM by Hoerl (1985) for cases where the objective of the optimization problem is different from the direction of convexity of the modeled function. The method considers a spherical constraint in x, assuming that, as an objective function, a second order polynomial model is adequate in some local region (Del Castillo, 2007; Meyers and Montgomery, 1995).

$$\begin{aligned}&Min \quad \hat{y} = b_0 + \mathbf{x}^{\mathbf{T}}\mathbf{b} + \mathbf{x}^{\mathbf{T}}\mathbf{B}\mathbf{x}\\&S.t. \therefore \mathbf{x}^{\mathbf{T}}\mathbf{x} \le \rho^2\end{aligned} \tag{11}$$

The constraint $\mathbf{x}^{\mathbf{T}}\mathbf{x} \le \rho^2$ refers to the experimental region and delimits the region to be optimized preventing optimization from occurring in the point where variance is high.
Lin and Tu (1995)proposed a non-linear optimization method that combines the mean, the variance and the target – optimal point for *y(x)*, using the minimization of mean square error – MSE. In that case, the MSE is the objective function subject to the experimental region constraint (Ardakani and Noorossana, 2008; De Paiva*et al.*, 2014; Shin*et al.*, 2011).

$$\begin{aligned}&Min \ MSE = (\hat{\mu} - T)^2 + \hat{\sigma}^2\\&S.t. \therefore \mathbf{x}^{\mathbf{T}}\mathbf{x} \le \rho^2\end{aligned} \tag{12}$$

On MSE approach may be used in situations in which the mean and the variance have to assume different degrees of importance. In that case, the MSE function can be modified considering weights ω_1 and$\omega_2$as positive constants previously specified (Linand Tu, 1995; Tang and Xu, 2002). The weights can be tried from different convex combinations that consider $\omega_1 + \omega_2 = 1$, $\omega_1 > 0$ e $\omega_2 > 0$. The weights can be varied to generate a set of non-inferior solutions for this multi-objective optimization problem(Tang and Xu, 2002).This optimization problem is exposed on Eq. (13).

Considering that in the multi-criteria optimization task no single optimal point x* would usually minimize every objective function simultaneously, there is a fundamental concept known for Pareto Optimality which is useful in the multi-objective approach (Das and Dennis, 1996).On multi-objective MSE optimizationthere is a common concern related to the convexity of Pareto frontiers generated, using weighted sums(Brito *et al.*, 2014).

$$\begin{aligned}&Min_{x \in \Omega} MSE = \omega_1 (\hat{\mu} - T)^2 + \omega_2 \hat{\sigma}^2\\&S.t. \therefore \mathbf{x}^{\mathbf{T}}\mathbf{x} \le \rho^2;\\&\omega_1 + \omega_2 = 1\\&\omega_1 > 0\\&\omega_2 > 0\end{aligned} \tag{13}$$

The Normal Boundary Intersection – NBI method, developed by Das and Dennis (1996), offer uniformly spread Pareto optimal solutions for a general non-linear multi-objective optimization problem (Shukla and Deb, n.d.).

According toBrito *et al.* (2014), establishing the payoff matrix *Φ* is the first step of the NBI method. It is based on the individual optimization of each objective function. Considering $F_z(x)$and $\hat{\sigma}^2(x)$ the objective functions for mean and variance, respectively, in matrix notation, the payoff matrix *Φ* for a bi-objective optimization problem can be written as:

$$\phi = \begin{bmatrix} F_z^*(x_1^*) & F_z(x_1^*) \\ \hat{\sigma}^2(x_2^*) & \hat{\sigma}^{2*}(x_2^*) \end{bmatrix} \tag{14}$$

Each row of the payoff matrix *Φ* is composed of minimum and maximum values of the objective functions. The solution that minimizes each objective function, i.e., the utopia points for$F_z(x)$and $\hat{\sigma}^2(x)$are, respectively,$F_z^*(x_1^*)$and $\hat{\sigma}^{2*}(x_2^*)$. The maximum values for$F_z(x)$and$\hat{\sigma}^2(x)$, called nadir points are, respectively, $F_z(x_1^*)$and$\hat{\sigma}^2(x_2^*)$.

Out of these values, the objective functions can be normalized. The objective functions normalization can be obtained using these two sets:

$$\overline{F}_z(x) = \frac{F_z(x) - F_z^*(x_1^*)}{F_z(x_1^*) - F_z^*(x_1^*)} \tag{15}$$

$$\overline{\hat{\sigma}}(x) = \frac{\hat{\sigma}^2(x) - \hat{\sigma}^{2*}(x_2^*)}{\hat{\sigma}^2(x_2^*) - \hat{\sigma}^{2*}(x_2^*)} \tag{16}$$

For bi-dimensional problems, the NBI-MSE optimization problem can be written as:

$$\begin{aligned} &Min \quad \bar{F}_z(x) \\ &S.t.: \quad \bar{F}_z(x) - \bar{\hat{\sigma}}(x) + 2w - 1 = 0 \\ &\qquad\quad \mathbf{x}^\mathrm{T}\mathbf{x} \le \rho^2 \end{aligned} \tag{17}$$

Ardakani and Noorossana (2008) discussed different optimization techniques for multi-objective decision-making, among them the MSE method.Shin *et al.*(2011) addressed a bi-objective robust design problem from which a Pareto frontier was obtained. De Paiva *et al.*, (2014) considered a multi-objective approach combining RSM and Principal Component Analyses – PCA to study a multi-response dataset with an incorporated noise, using a DOE combined array. De Motta *et al.* (2012) tested several procedures to deal with multi-objective optimization problems, among them the NBI method.

4. EXPERIMENTAL PROCEDURE

To achieve the purpose of this study, 26 experiments were carried out in a helical milling operation of Al-alloy 7075. The experiments were conducted on a *ROMI Discovery 560* (CNC lathe), with the maximum rotational speed and power of 10.000 rpm and 15 kW, respectively, equipped with a numerical control *Siemens 810D Sinumeric* model. It was used a 10 mm diameter solid carbidendmill with a 4-tooth and 30° helix angle. The cylindrical workpieces, with dimensions of 23mm diameter and 14mm height, were machined considering three control variables: cutting speed (v_c, m/min), axial feed per tooth (f_{za}, mm/min) and tangential feed per tooth (f_{zt}, mm/min) and one noise variable: tool length (l_b, mm). The use of a noise variable aims to obtain a robust parameter design for the surface F_z(N).

A stationary piezoeletric dynamometer with four *Kistler 9272* components, with signal amplifier and dedicated software, was used to measure the machining force component F_z.

The present work may be summarized in the following procedures:

Step 1: Experimental design: Draws up a combined array as an experimental design, considering control variables and noise variable. Runs the trials in a random order, does roughness measurements and store de responses.

Step 2: Modeling of responses including control and noise variables: Defines equation for $F_z(x,z)$using the measured responses.

Step 3: Definition of mean and variance equations: From $F_z(x,z)$ defines $F_z(x)$and $\hat{\sigma}^2(x)$equations and plots their surfaces.

Step 4: Constrained optimization of NBI-MSE: Establishes the response targets through the individual optimization of $F_z(x)$and $\hat{\sigma}^2(x)$equations. Defines the payoff matrix. Normalizes the $F_z(x)$and $\hat{\sigma}^2(x)$equations. Executes NBI - MSE optimization, considering different weights.

Step 5: Plot Pareto Frontier: Plots the Pareto frontier using NBI-MSE method.

5. RESULTS AND DISCUSSIONS

Step 1: Experimental design: The experimental design considering control and noise variables and the stored responses are detailed on Table 1.

Step 2: Modeling of responses including control and noise variables: Equation (18) presents the response modelin coded units for surface F_z.The model was obtained through WLS,and presented a good adjustment with $R^2 = 98.33\%,\ R^2_{adj} = 96.52\%,\ R^2_{pred} = 83.79\%$, and no lack-of-fit (LOF), once the p-value for LOF test was 0.415.

$$\begin{aligned} F_z(x,z) = {} & 242{,}575 + 43{,}100 f_{za} + 7{,}049 f_{zt} + 2{,}905 v_c + 5{,}151 l_b - 9{,}472 f_{za}^2 - 7{,}663 f_{zt}^2 - 7{,}882 v_c^2 - 6{,}001 f_{za} \times f_{zt} + \\ & 2{,}000 f_{za} \times v_c - 4{,}612 f_{za} \times l_b + 0{,}393 f_{zt} \times v_c - 3{,}480 f_{zt} \times l_b - 1{,}946 v_c \times l_b \end{aligned} \tag{18}$$

Step 3: Definition of mean and variance equations: Equations(19)and (20) presents, respectively,mean and variance models for surface F_z.Figure (2) shows the response surfaces for mean and variance of F_z, considering f_{zt} and v_c control factors.

$$\begin{aligned} F_z(x) = {} & 242{,}575 + 43{,}100 f_{za} + 7{,}049 f_{zt} + 2{,}905 v_c - 9{,}472 f_{za}^2 - 7{,}663^2_{fzt} - 7{,}882 v_c^2 - 6{,}001 f_{za} \times f_{zt} + 2{,}000 f_{za} \times v_c \\ & + 0{,}393 f_{zt} \times v_c \end{aligned} \tag{19}$$

$$\sigma^2(x) = (5{,}151 - 4{,}612 f_{za} - 3{,}480 f_{zt} - 1{,}946 v_c)^2 + 1{,}111 \tag{20}$$

Table 1. Experimental design

RunOrder	ControlFactors			Noise	Response
	f_{za}[mm/tooth]	f_{zt} [mm/tooth]	v_c[m/min]	l_b [mm]	F_z [N]
1	0.004	0.04	30	30	146.93
2	0.011	0.04	30	30	249.16
3	0.004	0.09	30	30	183.51
4	0.011	0.09	30	30	273.74
5	0.004	0.04	70	30	186.48
6	0.011	0.04	70	30	262.96
7	0.004	0.09	70	30	188.73
8	0.011	0.09	70	30	271.89
9	0.004	0.04	30	46	188.44
10	0.011	0.04	30	46	265.92
11	0.004	0.09	30	46	215.08
12	0.011	0.09	30	46	254.12
13	0.004	0.04	70	46	174.22
14	0.011	0.04	70	46	266.21
15	0.004	0.09	70	46	198.05
16	0.011	0.09	70	46	272.59
17	0.0005	0.065	50	38	29.88
18	0.0145	0.065	50	38	287.62
19	0.0075	0.015	50	38	176.39
20	0.0075	0.115	50	38	193.89
21	0.0075	0.065	10	38	171.02
22	0.0075	0.065	90	38	197.47
23	0.0075	0.065	50	38	228.40
24	0.0075	0.065	50	38	242.73
25	0.0075	0.065	50	38	226.60
26	0.0075	0.065	50	38	227.79

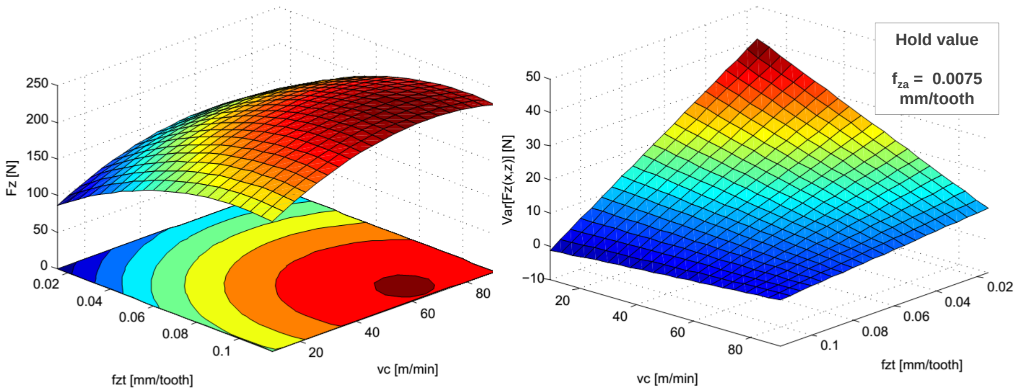

Figure 2. Response surface plots for $F_z(x)$and $\hat{\sigma}^2(x)$ considering v_c and f_{zt}

Step 4: Constrained optimization of NBI-MSE: The individual optimization of $F_z(x)$and $\hat{\sigma}^2(x)$ conducted to the respective optimal values: $\xi_{F_z} = 138.678$Nand$\xi_{\sigma^2} = 1{,}111$ N.After the individual optimization, the utopia and nadir points lead to the payoff matrix exposed on Table 2.

Table 2. Payoff matrix

138.678	266.626
205.490	**1.111**

Considering the utopia and nadir points, the different weights - Eq. (15) and (16), the normalization, and the NBI-MSE procedure - Eq. (17), the optimization results are resumed on Table 3.

Step 5: Plot Pareto Frontier: Through the NBI-MSE optimization, considering different weights, a Pareto Frontier using NBI-MSE approach was plottedas displayed on Fig. (3a).

The MSE approach was used to obtain a set of Pareto optimal solutions for mean and variance of F_z, Fig. (3b), and, in contrast to NBI method, it did not offer a uniformly spread Pareto optimal solutions for a non-linear multi-objective optimization problem.

Table 3. NBI-MSE optimization results

ω	Controlfactors			Responses		
	f_{za}[mm/tooth]	f_{zt} [mm/tooth]	v_c [m/min]	$F_z\ (x)$ [N]	$\hat{\sigma}^2(x)$ [N]	*WMSE* [N]
0	0.641	0.491	0.253	266.626	1.111	1.111
0.05	0.300	0.840	0.434	253.831	1.111	664.064
0.1	0.025	1.103	0.615	241.036	1.111	1048.719
0.15	-0.210	1.318	0.785	228.242	1.111	1204.187
0.2	-0.448	1.269	1.008	215.887	1.814	1193.699
0.25	-0.666	1.135	1.047	205.786	6.116	1130.441
0.3	-0.835	1.008	1.056	197.270	12.952	1038.972
0.35	-0.973	0.888	1.045	189.819	21.487	929.353
0.4	-1.089	0.773	1.023	183.154	31.278	809.994
0.45	-1.188	0.663	0.988	177.108	42.058	687.704
0.5	-1.274	0.557	0.945	171.575	53.659	567.931
0.55	-1.350	0.455	0.894	166.485	65.966	454.964
0.6	-1.416	0.354	0.836	161.792	78.906	352.095
0.65	-1.473	0.256	0.770	157.464	92.431	261.725
0.7	-1.522	0.157	0.697	153.485	106.514	185.426
0.75	-1.563	0.059	0.617	149.854	121.151	123.956
0.8	-1.596	-0.041	0.527	146.581	136.362	77.239
0.85	-1.620	-0.145	0.428	143.702	152.200	44.279
0.9	-1.632	-0.253	0.315	141.285	168.777	22.991
0.95	-1.630	-0.372	0.182	139.480	186.332	9.927
1	-1.601	-0.514	0.015	138.678	205.490	0.000

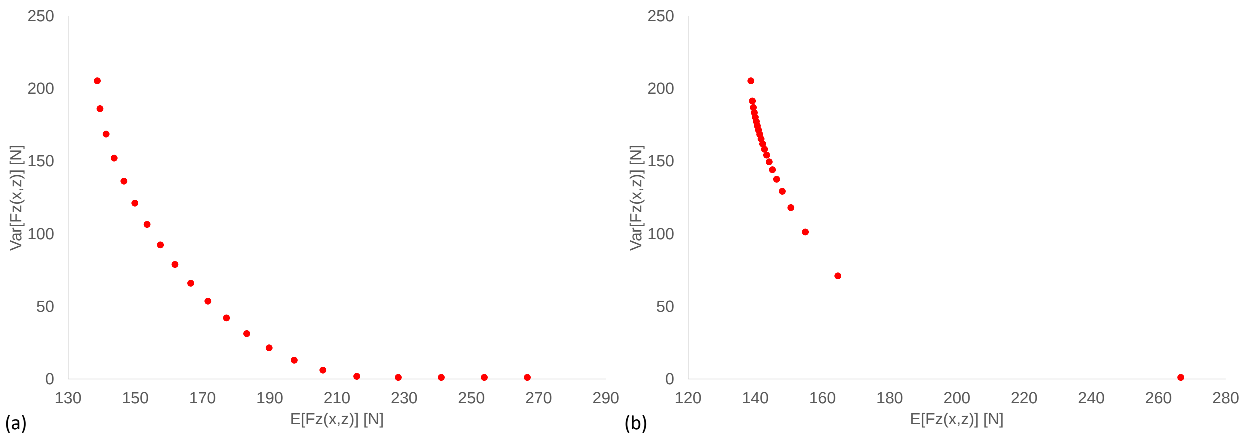

Figure 3. Pareto Frontiers for (a) NBI-MSE approach and (b) WMSE approach

6. CONCLUSION

In this paper it was shown the helical milling process as an alternative for drilling. Through a central composite design, a combined array considering control and noise factors, was elaborated, and after the experimental driving both the modeling and optimization of $F_z$machining force component were reached.

Both the NBI and MSE approach using the$F_z$non-linear optimization confirmed the capacity of NBI approach of generating equispaced Pareto Frontierfor a bi-objective robust design model, minimizing the machining force component F_z and its variance.

Throughthe methodology proposed, the machining force component F_z -the component that contributes mostly in percentage terms of machining force -was minimized, and it was maderobust to noise variation, i.e., tool length variation. The tool length, can be certainly considered as a noise factor, once in machining cavities, there are geometries that implies higher tool length, what can generate higher vibrationlevels and poor part quality.

Table 3 illustrates that a weight of 0 prioritizes the variance function optimization, while a weight of 1 prioritizes the mean function optimization. In accordance with this study, in future confirmation runs, setting f_{za} to -1.274 mm/tooth, f_{zt} to 0.557mm/tooth and v_c to 0.945m/min, in coded units, $F_z(x)$and $\hat{\sigma}^2(x)$must reach 171.575N and 53.659N, respectively.

7. ACKNOWLEDGEMENTS

The authors gratefully acknowledge CNPq, CAPES, and FAPEMIG for supporting this research and the technician Camilo Lellis dos Santos for machine tool operation.

8. REFERENCES

Ardakani, M. K., & Noorossana, R. (2008). A new optimization criterion for robust parameter design - The case of target is best. *International Journal of Advanced Manufacturing Technology*, *38*(9-10), 851–859. doi:10.1007/s00170-007-1141-6

Bhattacharyya, A., Schueller, J. K., Mann, B. P., Ziegert, J. C., Schmitz, T. L., Taylor, F. J., & Fitz-Coy, N. G. (2010). A closed form mechanistic cutting force model for helical peripheral milling of ductile metallic alloys. *International Journal of Machine Tools and Manufacture*, *50*(6), 538–551. doi:10.1016/j.ijmachtools.2010.03.003

Brito, T. G., Paiva, a. P., Ferreira, J. R., Gomes, J. H. F., & Balestrassi, P. P. (2014). A normal boundary intersection approach to multiresponse robust optimization of the surface roughness in end milling process with combined arrays. *Precision Engineering*, *38*(3), 628–638. doi:10.1016/j.precisioneng.2014.02.013

Das, I., & Dennis, J. (1996). Normal-Boundary Intersection: An Alternate Method for Generating Pareto Optimal Points in Multicriteria Optimization Problems, (96). doi:http://dx.doi.org/10.1137/S1052623496307510

De Motta, R. S., Afonso, S. M. B., & Lyra, P. R. M. (2012). A modified NBI and NC method for the solution of N-multiobjective optimization problems. *Structural and Multidisciplinary Optimization*, *46*(2), 239–259. doi:10.1007/s00158-011-0729-5

De Paiva, A. P., Gomes, J. H. F., Peruchi, R. S., Leme, R. C., & Balestrassi, P. P. (2014). A multivariate robust parameter optimization approach based on Principal Component Analysis with combined arrays. *Computers & Industrial Engineering*, *74*, 186–198. doi:10.1016/j.cie.2014.05.018

Denkena, B., Boehnke, D., & Dege, J. H. (2008). Helical milling of CFRP–titanium layer compounds. *CIRP Journal of Manufacturing Science and Technology*, *1*(2), 64–69. doi:10.1016/j.cirpj.2008.09.009

Lin, D. K. J., & Tu, W. (1995). Dual Response Surface Optimization. *Journal of Quality Technology*, 27(1), 34-39.

Hoerl, R. W., & Hoerl, R. W. (1985). Ridge analysis 25 years later. *American Statistician*, *39*(3), 186–192. doi:10.2307/2683926

Iyer, R., Koshy, P., & Ng, E. (2007). Helical milling: An enabling technology for hard machining precision holes in AISI D2 tool steel. *International Journal of Machine Tools and Manufacture*, *47*(2), 205–210. doi:10.1016/j.ijmachtools.2006.04.006

Li, Z., & Liu, Q. (2012). Surface topography and roughness in hole-making by helical milling. *The International Journal of Advanced Manufacturing Technology*, *66*(9-12), 1415–1425. doi:10.1007/s00170-012-4419-2

Qin, X., Gui, L., Li, H., Rong, B., Wang, D., Zhang, H., & Zuo, G. (2012). Feasibility Study on the Minimum Quantity Lubrication in High-Speed Helical Milling of Ti-6Al-4V. *Journal of Advanced Mechanical Design, Systems, and Manufacturing*, *6*(7), 1222–1233. doi:10.1299/jamdsm.6.1222

Sasahara, H., Kawasaki, M., & Tsutsumi, M. (2008). Helical Feed Milling with MQL for Boring of Aluminum Alloy. *Journal of Advanced Mechanical Design, Systems, and Manufacturing*, *2*(6), 1030–1040. doi:10.1299/jamdsm.2.1030

Shin, S., Samanlioglu, F., Cho, B. R., & Wiecek, M. M. (2011). Computing trade-offs in robust design: Perspectives of the mean squared error. *Computers and Industrial Engineering*, *60*(2), 248–255. doi:10.1016/j.cie.2010.11.006

Shukla, P. K., & Deb, K. (n.d.). On Finding Multiple Pareto-Optimal Solutions Using Classical and Evolutionary Generating Methods, 1–38.

Tang, L. C., & Xu, K. (2002). Response Surface Optimization. *October*, *34*(4), 437–447.

Tonshoff, H. K. I., Konig, I., Neises, A., & Aachen, R. (1994). Keynote Papers presented in the Scientific Technical Committees Machining of Holes Developments in Drilling Technology, *43*, 551–561.

Yicai, S., Ning, H. E., Liang, L. I., Xiaojie, Q. I. N., & Wei, Z. (2011). Orbital Milling Hole of Aerospace Al-Alloy with Big Pitch *, (50975141), 329–335. doi:10.1007/s12209